JACC: CLINICAL ELECTROPHYSIOLOGY VOL. 8, NO. 4, 2022

PUBLISHED BY ELSEVIER

VENTRICULAR ARRHYTHMIAS - DIAGNOSIS

Assessing Noninvasive Delineation of Low-Voltage Zones Using ECG Imaging in Patients With Structural Heart Disease

Adam J. Graham, PhD,[a,*] Michele Orini, PhD,[a,b,*] Ernesto Zacur, PhD,[c] Gurpreet Dhillon, PhD,[a] Daniel Jones, MRCP,[a] Sandeep Prabhu, PhD,[d] Francesca Pugliese, MD, PhD,[a] Martin Lowe, PhD,[a] Syed Ahsan, MD,[a] Mark J. Earley, MD,[a] Anthony Chow, MD,[a] Simon Sporton, MD,[a] Mehul Dhinoja,[a] Ross J. Hunter, PhD,[a] Richard J. Schilling, MD,[a] Pier D. Lambiase, PhD[a,b]

ABSTRACT

OBJECTIVES This study sought to assess the association between electrocardiographic imaging (ECGI) parameters and voltage from simultaneous electroanatomic mapping (EAM).

BACKGROUND ECGI offers noninvasive assessment of electrophysiologic features relevant for mapping ventricular arrhythmia and its substrate, but the accuracy of ECGI in the delineation of scar is unclear.

METHODS Sixteen patients with structural heart disease underwent simultaneous ECGI (CardioInsight, Medtronic) and contact EAM (CARTO, Biosense-Webster) during ventricular tachycardia catheter ablation, with 7 mapped epicardially. ECGI and EAM geometries were coregistered using anatomic landmarks. ECGI points were paired to the closest site on the EAM within 10 mm. The association between EAM voltage and ECGI features from reconstructed epicardial unipolar electrograms was assessed by mixed-effects regression models. The classification of low-voltage regions was performed using receiver-operating characteristic analysis.

RESULTS A total of 9,541 ECGI points (median: 596; interquartile range: 377-737 across patients) were paired to an EAM site. Epicardial EAM voltage was associated with ECGI features of signal fractionation and local repolarization dispersion ($N = 7$; $P < 0.05$), but they poorly classified sites with bipolar voltage of <1.5 mV or <0.5 mV thresholds (median area under the curve across patients: 0.50-0.62). No association was found between bipolar EAM voltage and low-amplitude reconstructed epicardial unipolar electrograms or ECGI-derived bipolar electrograms. Similar results were found in the combined cohort ($n = 16$), including endocardial EAM voltage compared to epicardial ECGI features ($n = 9$).

CONCLUSIONS Despite a statistically significant association between ECGI features and EAM voltage, the accuracy of the delineation of low-voltage zones was modest. This may limit ECGI use for pr-procedural substrate analysis in ventricular tachycardia ablation, but it could provide value in risk assessment for ventricular arrhythmias.
(J Am Coll Cardiol EP 2022;8:426–436) © 2022 by the American College of Cardiology Foundation.

From the [a]Barts Heart Centre, Barts Health National Health Service Trust, London, United Kingdom; [b]Institute of Cardiovascular Science, University College London, London, United Kingdom; [c]Institute of Biomedical Engineering, University of Oxford, Oxford, United Kingdom; and the [d]Department of Cardiology, The Alfred Hospital, Melbourne, Australia. *Drs Graham and Orini contributed equally to this work and are joint first authors.
The authors attest they are in compliance with human studies committees and animal welfare regulations of the authors' institutions and Food and Drug Administration guidelines, including patient consent where appropriate. For more information, visit the Author Center.

Manuscript received April 30, 2021; revised manuscript received November 12, 2021, accepted November 16, 2021.

ISSN 2405-500X/$36.00 https://doi.org/10.1016/j.jacep.2021.11.011

Ventricular tachycardia (VT) is associated with increased mortality in patients with structurally abnormal hearts.[1] During catheter ablation of VT, contact electroanatomic mapping (EAM) has been used to delineate the scar substrate necessary for the initiation and maintenance of ventricular arrhythmia. Bipolar and unipolar electrogram voltage can be used to differentiate normal tissue from dense scar and border zones.[2] Scar and border zone areas contain regions of conduction block and conduction slowing necessary for re-entrant circuits to form. In turn, these provide targets for ablation and are markers of arrhythmic risk.[3] Noninvasive scar assessment as an adjunct to standard substrate mapping during VT ablation has shown promise,[4,5] and the use of other noninvasive imaging modalities could offer further benefits.

Beyond the setting of VT ablation, more accurate methods for the noninvasive characterization of arrhythmogenic substrate in the ventricles are needed. Current clinical guidelines for the implantation of implantable cardioverter-defibrillators (ICDs) rely on reduced left ventricular (LV) ejection fraction (LVEF) to predict the risk of arrhythmic death.[6] This strategy has its limitations, with the majority of sudden cardiac deaths occurring in those with an LVEF of >35%.[7] Noninvasive delineation of scar is currently mainly based on cardiac magnetic resonance,[8,9] with infarct mass and area better at predicting arrhythmia than LVEF[10] and border zone scar characterization being correlated to ventricular arrhythmia in various cardiomyopathies.[11–13]

Electrocardiographic (ECG) imaging (ECGI) allows noninvasive assessment of cardiac electrical activity within 1 single beat by combining body surface ECG and cardiac imaging.[14] It has been used to assess electrophysiologic functional parameters such as activation time (AT) and repolarization time (RT) as well as critical sites of VT,[15–17] but there is a paucity of evidence examining its use for scar localization in humans.

In this study, we assessed low-voltage zone (as a standard surrogate for scar) delineation using a commercial system for ECGI (CardioInsight, Medtronic), which uses torso-heart geometries from computed tomography (CT) scans and body-surface ECGs from a bespoke multielectrode vest to reconstruct a unipolar electrogram over the epicardial surface. We considered previously published[14,18–21] and novel ECGI-based metrics, such as spatial heterogeneity of activation and repolarization, and derived bipolar electrograms, with a comparison made to voltage maps acquired during VT ablations using a contact EAM system (CARTO, Biosense-Webster) as ground truth data. We hypothesized that low-voltage zones on EAM could be associated with low-amplitude ECGI electrograms, signal fractionation, and increased local activation and repolarization dispersion.

METHODS

The study received ethical oversight and was approved by the Institutional Review Board, National Research Service Committee, London (14/LO/0360). Sixteen patients undergoing catheter ablation of VT were recruited for the study. All patients were scheduled for catheter ablation of VT on clinical grounds and gave their informed consent to participate in the research study.

ELECTROPHYSIOLOGIC STUDIES. Procedures were performed under conscious sedation using diamorphine and midazolam or general anesthetic. Access was obtained under ultrasonographic guidance using the Seldinger technique via the right femoral vein and/or right femoral artery. All patients were planned for endocardial access to the right ventricle (RV) or LV access via transseptal puncture or retrogradely via the aorta. A subxiphisternal puncture using a Tuohy needle, with fluoroscopic guidance, was used to access the epicardial space in 7 patients, using a previously described technique.[22]

Geometry was collected from the ascending, arch, and descending aorta for coregistration with ECGI (**Figure 1**). If arterial access was not part of the procedure, detailed geometry from either the RV outflow tract and the inferior and superior vena cava or the left atrium was collected.

An EAM (CARTO) of the endocardium of the RV or LV with or without epicardium was created during sinus rhythm or RV pacing. Electrograms were recorded using a multipolar catheter or by point-by-point mapping (PentaRay, Decapolar, or SmartTouch, Biosense-Webster). High-density EAM voltage maps created in the mapping system by projecting recorded voltage onto the detailed anatomic mesh were used as ground truth. Bipolar voltages of <1.5 mV and <0.5 mV were considered indicative of scar and dense scar, respectively.[23]

ECGI ANALYSIS. The ECGI analysis is summarized in **Figure 2**. Before catheter ablation, a 252-electrode vest (CardioInsight V3.1, Medtronic) was fitted for the recording of body surface potentials (sampling

ABBREVIATIONS AND ACRONYMS

AUC = area under the receiver operating characteristic curve

AT = activation time

ARI = activation recovery interval

CT = computed tomography

EAM = electroanatomic mapping

ECG = electrocardiogram

ECGI = electrocardiographic imaging

ICD = implantable cardioverter-defibrillator

IQR = interquartile range

LV = left ventricle

LVEF = left ventricular ejection fraction

rUEG = electrocardiographic imaging-reconstructed unipolar electrogram

ROC = receiver operating characteristic curve

RT = repolarization time

RV = right ventricle

VT = ventricular tachycardia

JACC: CLINICAL ELECTROPHYSIOLOGY VOL. 8, NO. 4, 2022
APRIL 2022:426–436

FIGURE 1 EAM-ECGI Alignment

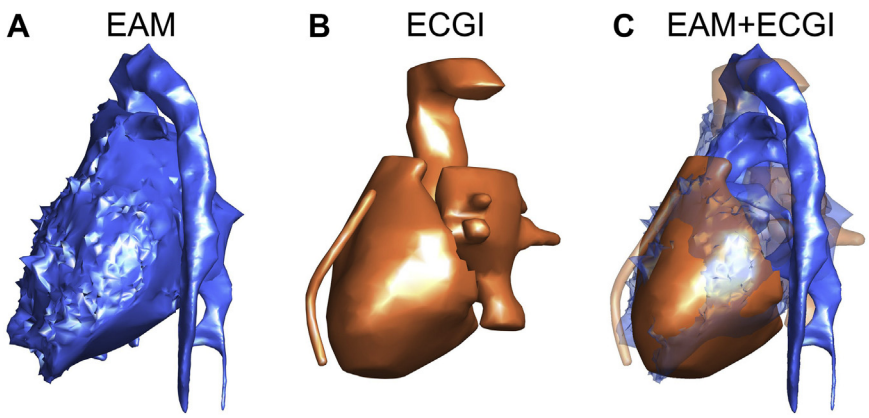

Anatomic coregistration of the **(A)** EAM and **(B)** ECGI geometries from 1 patient. **(C)** The 2 geometries are combined. Geometries are displayed in the left lateral view. EAM = electroanatomic mapping; ECGI = electrocardiographic imaging.

rate: 1,000 Hz) and remained in situ until the conclusion of the procedure. A noncontrast axial CT scan with 3-mm slice thickness was performed up to 4 hours before the procedure. Patient-specific epicardial geometry was created using the EcVue system (Medtronic), which utilizes heart-torso data from a CT scan of the patient's chest to produce an epicardial geometry of the ventricles and to localize individual electrodes on the 252-electrode vest. Signals recorded by the electrodes not seen on the CT scan or with insufficient quality according to propriety CardioInsight software are excluded. Reconstructed epicardial unipolar electrograms (rUEGs) are then computed using this geometric information by the CardioInsight system over approximately 1,400 epicardial points. rUEGs were computed from beats recorded during sinus rhythm or pacing. Electrograms over the atrioventricular valves were excluded from the analysis.

rUEGs were exported for offline analysis and bandpass filtered between 0.5 and 40 Hz after removing pacing artifacts. rUEGs were then analyzed for fractionation, which was measured as the number of negative deflections during the QRS complex (N_{Def}).[24,25] Peak-to-peak unipolar electrogram amplitude (A_{UNI}) was measured, and sites with amplitude lower than 15% ($A_{15\%}$) and 30% ($A_{30\%}$) of the largest A_{UNI} across all cardiac sites were identified for possible correlation with dense scar (<0.5 mV) and total scar zones (<1.5 mV) as in previous studies.[21] AT and RT were measured at the instant of minimum derivative during the QRS complex (dV/dt_{min}) and maximum derivative during the T-wave (dV/dt_{max}) following standard definitions.[26–28] rUEGs were further low-pass filtered with a cutoff frequency of 20 Hz before RT annotation. Activation recovery interval (ARI), a surrogate for action potential duration,[26,28] was measured as ARI = RT - AT. For each site of the ECGI epicardial geometry, the local spatial heterogeneity of the AT and ARI (H_{AT} and H_{ARI}, respectively) was measured as the maximum minus the minimum difference of AT and ARI, respectively, within a radius of 8 mm.[29,30] A virtual bipolar electrogram voltage was computed as the difference between the rUEGs at that site and the nearest site, and its peak-to-peak amplitude (A_{BI}) was measured. All signals were reviewed and semiautomatically corrected using bespoke graphical user interfaces developed in Matlab (MathWorks Inc). rUEGs were analyzed blindly to the EAM from the CARTO system.

COREGISTRATION AND ECGI-EAM COMPARISON. Coregistration of EAM and ECGI geometries was performed semiautomatically with bespoke software (Matlab) as described previously and allows the *x*-, *y*-, and *z*-coordinates of points from both systems to be paired for analysis.[16,31] The optimal coregistration was visually determined by 2 experts independent of subsequent analysis. Alignment of ECGI and EAM maps was supported using extracardiac landmarks, such as the ascending, arch, and descending portions of the aorta, inferior vena cava, and left atrium. After anatomic coregistration, epicardial points on the ECGI epicardial geometry (representing virtual recording sites) were paired to the nearest CARTO point within a radius of 10 mm. An ECGI point was excluded from further analysis if its distance to the nearest CARTO point was larger than 10 mm. Pairing

FIGURE 2 **ECGI Process and Comparison With EAM**

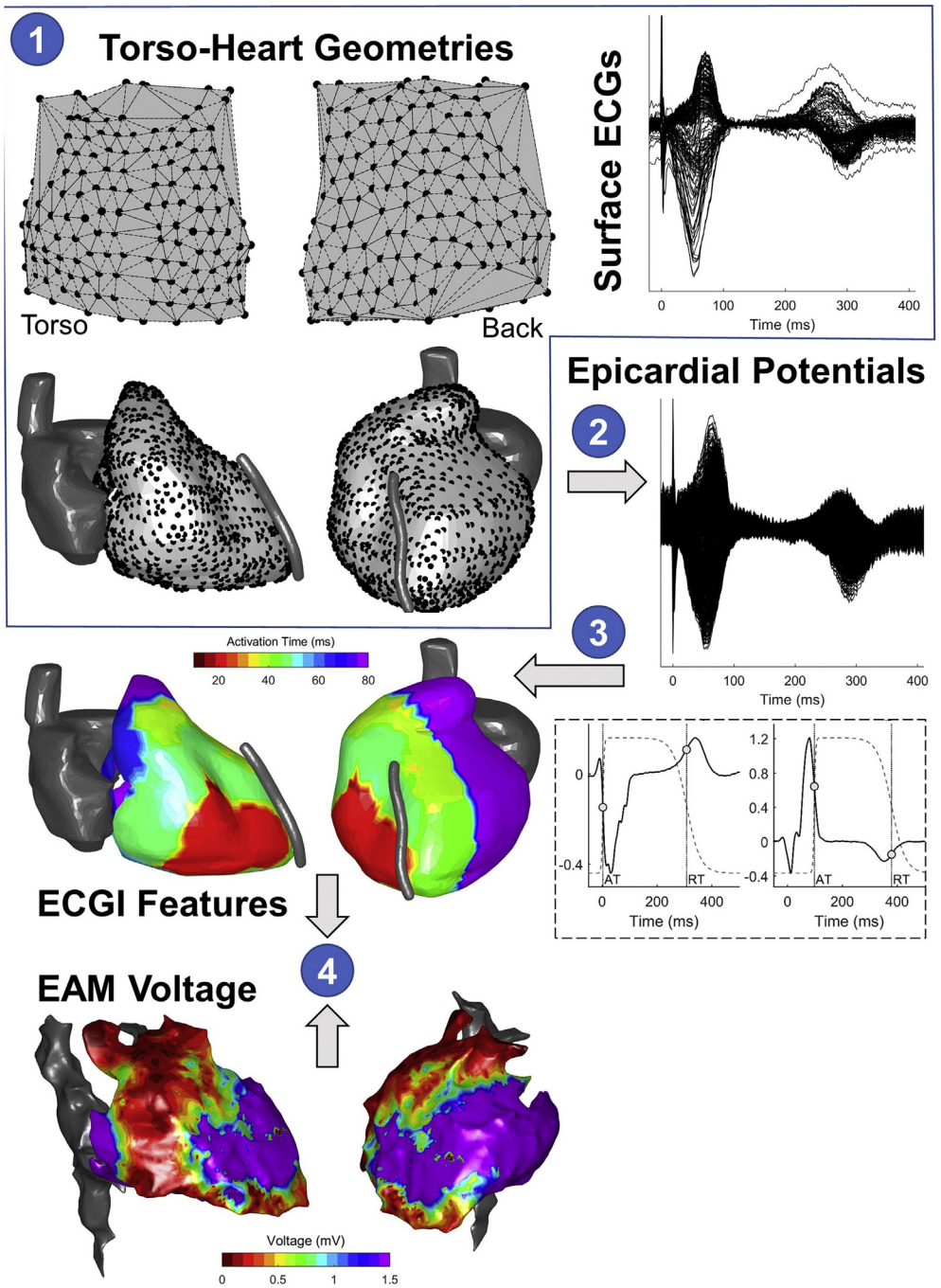

(1) Heart-torso geometries are derived from computed tomography, and body surface ECGs are recorded from 252 electrodes (black markers) on the CardioInsight vest. **(2)** The inverse problem of electrophysiology is solved, and epicardial unipolar potentials (rUEGs) are reconstructed at each epicardial site (**black markers**; usually 1,400). **(3)** rUEG amplitude, local AT and RT, signal fractionation, and virtual bipolar electrograms are derived from the rUEGs. AT and RT are measured using standard rules (with the relation between epicardial potentials and the action potential explained in the inset schematic). **(4)** ECGI and EAM cardiac geometries are coregistered, and cardiac sites from ECGI geometries are paired to the closest sites on the EAM. Finally, EAM voltage and low-voltage zones on EAM are compared to ECGI markers. AT = activation time; ECG = electrocardiogram; ECGI = electrocardiographic imaging; EAM = electroanatomic mapping; RT = repolarization time; rUEG = electrocardiogram imaging–reconstructed unipolar electrogram.

JACC: CLINICAL ELECTROPHYSIOLOGY VOL. 8, NO. 4, 2022
APRIL 2022:426–436

TABLE 1 Baseline Characteristics

Patient #	Age, y	Sex	Etiology	LVEF, %	Location	Paired ECGI Points, n (%)	Nodes on EAM Mesh
1	47	F	ARVC	57	Epi	715 (53)	5,955
2	73	M	DCM	24	Epi	1,037 (75)	49,135
3	22	M	DCM	38	Endo RV	641 (46)	9,111
4	54	M	ARVC	56	Endo RV	518 (37)	21,621
5	48	M	BrS	55	Epi	983 (71)	26,118
6	81	M	IHD	18	Endo LV	637 (45)	17,677
7	82	M	IHD	24	Endo LV	436 (32)	28,109
8	76	F	IHD	22	Endo LV	228 (16)	7,713
9	27	F	ARVC	58	Epi	1,043 (74)	27,355
10	78	M	IHD	15	Endo LV	390 (28)	27,223
11	78	M	IHD	14	Endo LV	364 (27)	8,483
12	69	M	IHD	20	Endo LV	291 (21)	9,408
13	52	F	ARVC	57	Epi	657 (47)	3,120
14	58	M	ARVC	21	Epi	758 (55)	6,795
15	21	M	DCM	40	Epi	555 (41)	21,840
16	84	M	IHD	26	Endo LV	288 (20)	7,770

Patient characteristics, including the etiology of the cardiomyopathy, LVEF, and type of EAM (epicardial or endocardial), are shown. The number of ECGI sites paired to an EAM point is reported as is the proportion over the total number of ECGI points (in parentheses).

ARVC = arrhythmogenic right ventricular cardiomyopathy; BrS = Brugada syndrome; DCM = dilated cardiomyopathy; EAM = electroanatomic mapping; ECGI = electrocardiographic imaging; Endo = endocardial; Epi = epicardial; F = female; IHD = ischemic heart disease; LV = left ventricle; LVEF = left ventricular ejection fraction; M = male; RV = right ventricle.

was performed to ensure that ECGI points were not paired with the same CARTO point. In the 9 patients where EAM was performed endocardially, epicardial ECGI points were paired with endocardial EAMs using the same criteria. We hypothesized that, since unipolar electrograms are affected by remote electrical activity, features from epicardial ECGI rUEGs could provide information about endocardial activity. This is supported by previous studies showing a correlation between endocardial unipolar EAM and epicardial scar[32] and that epicardial ECGI can localize endocardial VT exit sites.[31]

STATISTICAL ANALYSIS. The association between EAM voltage and features of ECGI rUEGs was assessed using random-intercept linear mixed-effects models, with the unipolar or bipolar EAM voltage as dependent variables, the features of ECGI rUEGs as independent variables representing fixed effects, and the intercept varying by patient. This type of model allows an efficient use of the data minimizing pseudoreplication and has been previously used in similar studies.[20] A significant association was identified if the effect size showed the expected direction based on physiology (positive for A_{UNI} and A_{BI} and negative for $A_{15\%}$, $A_{30\%}$, N_{Def}, H_{AT}, and H_{ARI}) with $P < 0.05$. Two-way analysis of variance tests with patients modeled as a random effect were conducted to assess the differences of each ECGI parameter in low-voltage versus non-low-voltage zones. The accuracy in identification of a low-voltage zone using features of ECGI rUEGs was assessed using receiver-operating characteristic (ROC) curves. An ROC curve per patient was estimated, and the identification of low-voltage zones was assessed measuring the area under the ROC curve (AUC) at the individual level.

ECGI features with a significant association with bipolar EAM voltage were utilized in multivariable logistic models for the classification of dense (V <0.5 mV vs V ≥0.5 mV) or all (V <1.5 mV vs V ≥1.5 mV) scar. A logistic model per patient was identified, and accuracy was assessed as the median AUC across all patients. Since 1 logistic model is fitted per patient, results represent the best-case scenario where patient-specific models are used. Although logistic regressions require observation to be independent of each other, some degree of correlation in the electrophysiologic properties of adjacent cardiac sites may be expected. The classification results from patients with <5% of all points within either class were not included in the summary statistics.

Data distribution is described by median (interquartile range [IQR]). Statistical differences were assessed using the Wilcoxon rank sum test for unpaired comparisons and the Wilcoxon signed rank test for paired comparisons. Statistical analysis was performed in Matlab.

RESULTS

Baseline characteristics of all patients (n = 16) are described in Table 1. All patients had ECGI and EAM performed. EAMs were collected from the endocardium in 9 patients and from the epicardium in 7. Across the 16 patients, the median number of body surface ECG leads used to compute rUEGs was 185 (IQR: 175-206). Across all patients, 9,541 ECGIs and the endocardial and/or epicardial EAM sites were paired (median: 596; IQR: 377-737 across patients). The median proportion of ECGI sites paired to an EAM site was 43% per patient, with an IQR between 28% and 54% (Table 1). ECGI points were excluded from the analysis if their distance from the nearest CARTO point was >10 mm. Of all EAM paired points, 66% (IQR: 43%-81%) and 26% (IQR: 15%-43%) had a V of <1.5 and <0.5 mV on EAM, respectively. The median distance between the ECGI and EAM paired point was 4.3 (IQR: 3.1-5.6) mm.

ASSOCIATION BETWEEN EAM VOLTAGE AND ECGI FEATURES. Comparison of epicardial EAM voltage with epicardial ECGI maps (n = 7) showed that ECGI markers of signal fractionation (N_{Def}) and local

TABLE 2 Correlation Between Bipolar Electroanatomic Mapping Voltage and Electrocardiographic Imaging Parameters Assessed Using a Mixed-Effects Model

	Epicardial Patients (n = 7)	Epicardial (n = 7) + Endocardial (n = 9) Patients
A_{BI}	-0.90 (-1.18 to -0.61)	-0.85 (-1.08 to -0.61)
A_{UNI}	-0.08 (-0.10 to -0.05)	-0.05 (-0.07 to -0.03)
$A_{15\%}$	0.03 (-0.12 to 0.18)	-0.04 (-0.18 to 0.09)
$A_{30\%}$	0.25 (0.14 to 0.37)	-0.04 (-0.18 to 0.09)
N_{Def}	-0.15 (-0.18 to -0.12)[a]	-0.16 (-0.19 to -0.13)[a]
H_{ARI}	-0.004 (-0.005 to -0.003)[a]	-0.003 (-0.004 to -0.002)[a]
H_{AT}	-0.002 (-0.004 to 0.001)	-0.003 (-0.005 to -0.002)[a]

Values are effect size (95% CI). [a]Statistically significant interaction ($P < 0.05$), and the direction of the interaction is consistent with the hypothesis.

$A_{15\%}$ = peak-to-peak unipolar amplitude on ECGI lower than 15%; $A_{30\%}$ = peak-to-peak unipolar amplitude on ECGI lower than 30%; A_{BI} = peak-to-peak signal amplitude of ECGI bipolar electrogram; A_{UNI} = peak-to-peak signal amplitude of ECGI unipolar electrogram; H_{ARI} = local spatial heterogeneity of activation recovery interval; H_{AT} = local spatial heterogeneity of activation time; N_{Def} = number of negative deflections in the unipolar electrogram.

repolarization dispersion (H_{ARI}) were significantly associated with unipolar and bipolar EAM voltage, but with a low effect size (Table 2, Supplemental Table 1). Analysis of variance showed that N_{Def} and H_{ARI} were higher in sites with voltage of <1.5 mV than voltage of >1.5 mV ($P < 0.01$ for all comparisons) as well as in sites with V of <0.5 mV than V of >0.5 mV ($P < 5 \times 10^{-5}$ for all comparisons). The amplitude of the ECGI unipolar and bipolar rUEGs was not significantly associated with EAM voltage (Table 2, Supplemental Table 1).

Comparison of endocardial EAM voltage (n = 9) with epicardial ECGI showed similar results (Supplemental Table 2). When comparing EAM voltage from both endocardial (n = 9) and epicardial (n = 7) maps with epicardial ECGI maps, bipolar EAM voltage remained significantly associated with ECGI features of rUEG fractionation and local dispersion of repolarization, as well as with local dispersion of AT (Table 2).

TABLE 3 Identification of Low-Voltage Zones

	Epicardial (n = 7)		Epicardial (n = 7) + Endocardial (n = 9)	
	V <0.5 mV	V <1.5 mV	V <0.5 mV	V <1.5 mV
N_{Def}	54 (51-60)	53 (50-56)	58 (53-62)	55 (51-62)
H_{ARI}	53 (49-55)	57 (53-59)	55 (49-58)	57 (51-60)
H_{AT}	–	–	53 (48-57)	54 (49-55)

Values are median (interquartile range) of the percent area under the receiver-operating characteristic curve measuring the accuracy of low electroanatomic mapping voltage localization using electrocardiogram imaging , with V of <0.5 mV and <1.5 mV, respectively.

Abbreviations as in Table 2.

DISCRIMINATION OF EAM LOW-VOLTAGE ZONES. Discrimination of low-voltage sites based on ECGI parameters was poor, with median value of the AUC across patients was ≤0.58 (Table 3). The multivariable model based on combining the ECGI features of fractionation (N_{Def}) and repolarization local heterogeneity (H_{ARI}) identified sites with EAM bipolar voltage <0.5 mV and <1.5 mV with an AUC of 0.64 (IQR: 0.59-0.67) and AUC of 0.63 (IQR: 0.61-0.76), respectively (median and IQR across the combined cohort of endocardial and epicardial patients). Sensitivity and specificity, calculated using patient-specific thresholds optimizing accuracy, varied considerably across patients, with median values ranging between 60% and 70%.

Figure 3 shows EAM and ECGI scar maps from all epicardial patients. In the EAM (left side), scar was identified as bipolar voltage of <1.5 mV, whereas in the ECGI map (right side), scar was identified as the output of the multivariable logistic regression using the cutoff value that maximized sensitivity and specificity. In most patients, qualitatively, the 2 maps show a similar pattern. However, quantitative assessment showed low point-by-point agreement, with AUC ranging between 0.57 and 0.62.

DISCUSSION

This is the first study, to our knowledge, to assess the ability of the novel ECGI CardioInsight system to localize low-voltage zones in patients with structural heart disease and VT (Central Illustration). Comparison with simultaneous EAM has demonstrated that ECGI markers of signal fractionation (N_{Def}) and local activation and repolarization heterogeneity (H_{AT} and H_{ARI}, respectively) were significantly associated with low-voltage zones delineated using contact EAM. However, the capability of these features to discriminate low-voltage zones was limited (median AUC: ≤0.58). Integration of these 3 ECGI features did not dramatically improve low-voltage zone localization. The amplitude of rUEGs and ECGI-derived bipolar electrograms showed no association with low-voltage zones. Of note, although in a previous study we demonstrated good agreement between the morphology of EAM-recorded and rUEGs,[16] in this study, the amplitude of rUEGs was not significantly associated with EAM unipolar voltage. This suggests that CardioInsight may be able to reproduce signals that present similar morphology as that recorded with contact mapping, but with different amplitudes (ie, with a nonconstant scaling factor across cardiac sites).

JACC: CLINICAL ELECTROPHYSIOLOGY VOL. 8, NO. 4, 2022
APRIL 2022:426–436

FIGURE 3 EAM-ECGI Agreement on Epicardial Maps

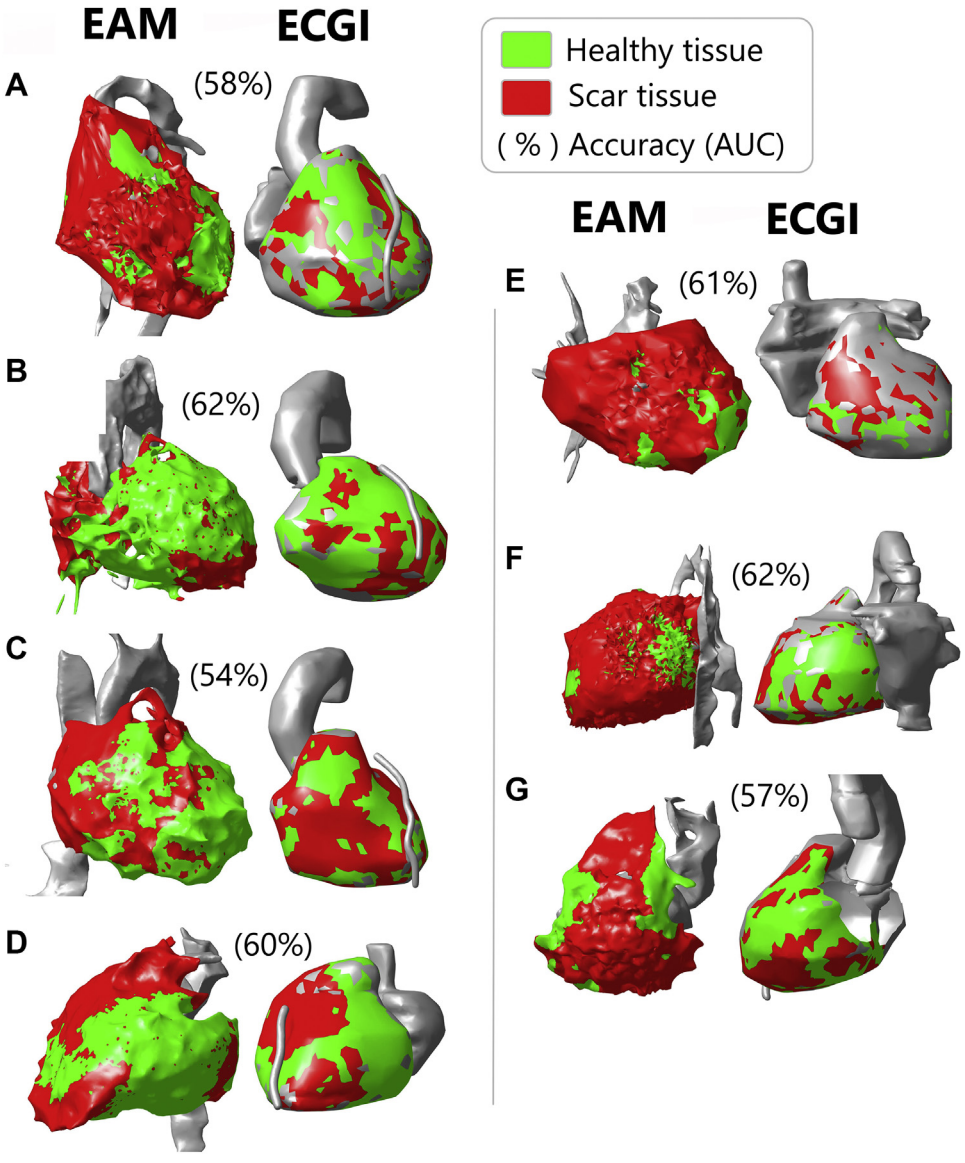

Comparison between scar maps derived from voltage EAM and ECGI. In EAM, scar and healthy tissues are defined as bipolar voltage V of <1.5 ms and >1.5 mV, respectively. In ECGI maps, scar and healthy tissues are identified based on a logistic model including parameters measuring signal fractionation (N_{Def}) and repolarization heterogeneity (H_{ARI}). The cutoff value for discriminating between scar and healthy tissue was determined using ROC analysis on a case-by-case bases. Accuracy is measured as the area under the receiver-operating characteristic curve and is reported in brackets. Shown are patients **(A)** 1, **(B)** 2, **(C)** 5, **(D)** 9, **(E)** 13, **(F)** 14, and **(G)** 15 (Table 1). Abbreviations as in Figure 2.

A significant association between features of rUEGs and EAM voltage was not only found in patients for whom contact mapping was conducted on the epicardium (n = 7) but also for patients for whom contact mapping was conducted on the endocardium (n = 9). This may be due to the effect of remote electrical activity on the morphology of the unipolar electrograms,[27] which has been previously used to identify epicardial scar using endocardial unipolar mapping.[32]

Studies assessing the capability of ECGI to detect scar are limited in number. Using an infarcted canine heart, the initial pioneers of the technology showed that morphologic characteristics of the ECGI

CENTRAL ILLUSTRATION **Noninvasive Delineation of Low-Voltage Zones Using ECGI in VT Patients**

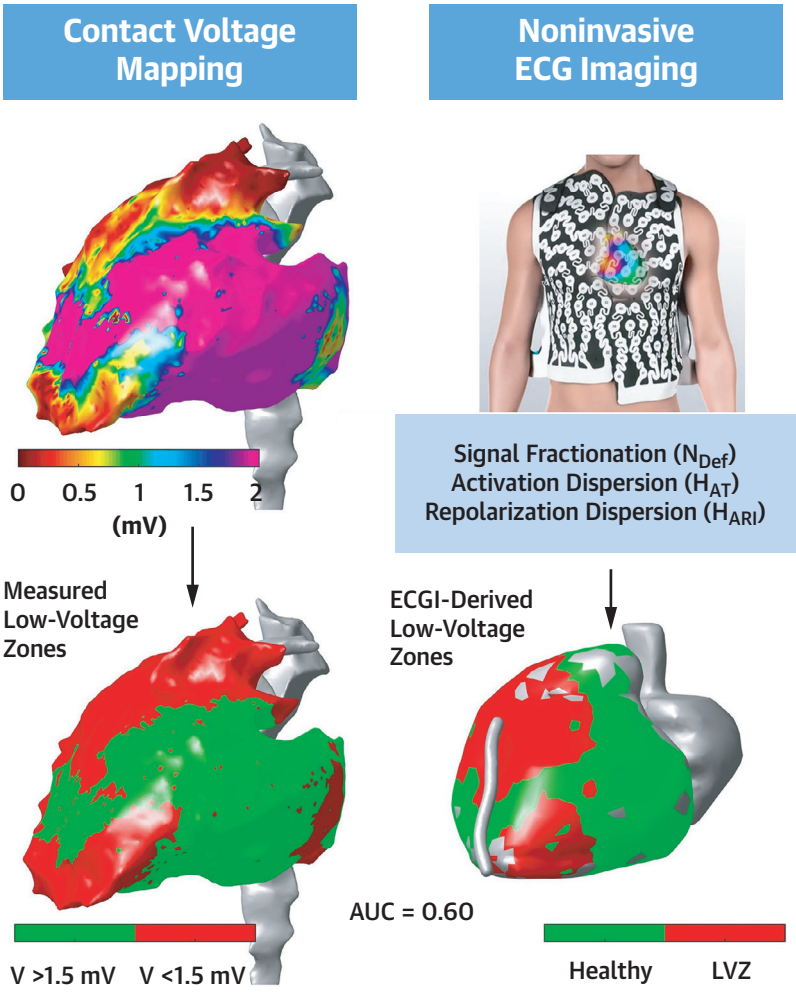

Graham AJ, et al. J Am Coll Cardiol EP. 2022;8(4):426-436.

AUC = area under the receiver operating characteristic curve; ECGI = electrocardiographic imaging; H_{ARI} = local spatial heterogeneity of activation recovery interval; H_{AT} = local spatial heterogeneity of activation time; LVZ = low-voltage zone; NDef = number of negative deflections in the unipolar electrogram; VT = ventricular tachycardia.

electrograms corresponded to areas of anatomic scar.[18] The same research group expanded on this by testing the hypothesis that ECGI could characterize myocardial scar. Cuculich et al[14] used ECGI maps created during sinus rhythm to characterize electrical scar and used cardiac magnetic resonance and myocardial perfusion imaging as a reference. Late potentials, lines of block, fractionation, and low unipolar voltage (defined as follows: <30% of maximum unipolar amplitude was denoted as low voltage and <15% as very low voltage) were associated with scar areas. Using the standard 17-segment American Heart Association model, ECGI colocalized scar with a sensitivity of 89% and a specificity 85%. This contrasts with the findings in our study. Differences may, in part, be ascribed to the use of different inverse problem solutions[33,34] and the use of noninvasive imaging, as opposed to EAM, for the identification of ground truth electrophysiologically defined scar with higher mapping resolution. Furthermore, the present study attempted to assess the capacity of ECGI to localize

JACC: CLINICAL ELECTROPHYSIOLOGY VOL. 8, NO. 4, 2022
APRIL 2022:426–436

low-voltage zones at the spatial level of each single cardiac site, whereas previous studies had focused on the localization of scar in large cardiac segments.[14] The findings in this study reflect the limitations of inverse solution algorithms to fully compensate for factors that influence epicardial signal amplitudes, such as individual variations in body habitus, chest wall impedance caused by adipose tissue, and lung air. The most contemporary study to investigate associations with scar used ECGI signal features derived from a 120-lead research system to identify low-voltage zones in 4 patients.[20] Qualitatively, there was overlap between scar on contact mapping and ECGI with dense scar, with more discordance seen with heterogenous scar. However, sensitivity and specificity were modest and in line with the results of our study.

In this study, we used low EAM voltage as a reference for abnormal tissue because this is standard practice in electrophysiologic study. However, bipolar voltage can be affected by wavefront directionality and catheter configuration[35] as well as wall thickness,[36] which may invalidate universal voltage thresholds for the localization of scar.

The significant associations between some ECGI parameters with low-voltage zones documented in this study may enable its use as a risk stratification tool in patients with structurally abnormal hearts. Indeed, ECGI parameters were shown to correlate with the burden of fibrosis at the patient level,[24] and a recent study used ECGI to differentiate the electrophysiologic substrate of patients with ICDs who had received therapies compared with a primary prevention cohort who had never received shocks.[21] The ICD therapy group had a significantly greater burden of electrical scar, more late potentials, and greater fractionation, which offers potential for ECGI's use in risk stratification. Indeed, recent studies of conduction stability using ECGI point toward its application in this area.[37] Therefore, it could provide clinical data to supplement the current use of LVEF measurement with the potential to be combined with other biomarkers in risk stratification for ICD implantation. This would require prospective studies to establish.

The use of EAM in substrate-based ablation of VT is common, and the use of noninvasive technology to localize scar has shown utility in this setting.[4] Our data suggest that currently, ECGI lacks sufficient resolution in scar localization to aid in these procedures. Our previous work has demonstrated that it outperforms the 12-lead ECG in the localization of VT exit sites.[31] However, further advances in the technology would be necessary for its routine use as an adjunct to substrate-based ablation procedures.

STUDY LIMITATIONS. The ECGI CardioInsight system is designed for creation of AT maps for the expedient mapping of ventricular arrhythmia,[38] and in its current version, it is not marketed to assess location or burden of scar. Therefore, the use of specific inverse problem solutions may improve accuracy. Our previous work demonstrated that ECGI showed more clinical utility for mapping ATs.[16,31] The system is purported to reconstruct epicardial electrograms and does not include the septum. Therefore, no inference can be made on data presented here regarding septal low-voltage zones. Furthermore, the cohort of patients included is heterogeneous in that we included patients with cardiomyopathies with differing etiologies and distributions of scar. The study was designed to assess the capability of ECGI to localize low-voltage zones independent from scar etiology. However, it is plausible that it may be better able to localize more confluent scar due to prior myocardial infarction.

Although the data were collected simultaneously, there may be some variation beat to beat. The EAM consists of many beats collected over several minutes, and ECGI uses a single beat. Although all beats were carefully aligned offline with custom software and manually checked, variation in the reconstructed electrograms may have occurred.

Prior work from our group has demonstrated the importance of the accurate coregistration of geometries. We found that a ±25% variation in the correlation of AT maps between ECGI and EAM, with small variations in the anatomic coregistration.[16] However, we believe that the use of anatomic landmarks minimizes misalignment.[39]

CONCLUSIONS

This study showed that ECGI electrogram features of signal fractionation and local activation and repolarization heterogeneity were significantly associated with low-voltage zones, but their accuracy in delineating the spatial distribution of scar was modest. This may limit its use for preprocedural substrate analysis in VT ablation. These shortcomings may be addressed by further innovations in the algorithms for solving the inverse equation and signal processing methods.

FUNDING SUPPORT AND AUTHOR DISCLOSURES

Dr Graham was supported by a Barts Charity grant. Dr Lambiase was supported by University College London Hospital Biomedicine National Institute for Health Research and Barts Biomedical Research Centre; has received research grants from Boston Scientific, Medtronic, and Abbott; and has received speaker fees from Medtronic. All other authors have reported that they have no relationships relevant to the contents of this paper to disclose.

ADDRESS FOR CORRESPONDENCE: Dr Pier D. Lambiase, University College London, Institute of Cardiovascular Science and Cardiology Department, Barts Heart Centre, Barts Health NHS Trust, West Smithfield, London EC1A 7BE, United Kingdom. E-mail: p.lambiase@ucl.ac.uk.

PERSPECTIVES

COMPETENCY IN MEDICAL KNOWLEDGE: ECGI can be used as an adjunct to noninvasive ablation of VT. Current data suggest it possesses insufficient resolution to localize scar. Therefore, its utility in substrate-based ablation would be limited to the mapping of hemodynamically nontolerated VT.

TRANSLATIONAL OUTLOOK: The finding of statistically significant associations between ground truth data and ECGI markers of scar needs further prospective study to assess if these can be used as markers of arrhythmia risk.

REFERENCES

1. Bigger JT, Fleiss JL, Kleiger R, Miller JP, Rolnitzky LM. The relationships among ventricular arrhythmias, left ventricular dysfunction, and mortality in the 2 years after myocardial infarction. *Circulation*. 1984;69(2):250–258.

2. Josephson ME, Anter E. Substrate mapping for ventricular tachycardia assumptions and misconceptions. *J Am Coll Cardiol EP*. 2015;1(5):341–352.

3. Graham AJ, Orini M, Lambiase PD. Limitations and challenges in mapping ventricular tachycardia: new technologies and future directions. *Arrhythmia Electrophysiol Rev*. 2017;6(3):118–124.

4. Andreu D, Penela D, Acosta J, et al. Cardiac magnetic resonance–aided scar dechanneling: influence on acute and long-term outcomes. *Heart Rhythm*. 2017;14(8):1121–1128.

5. Soto-Iglesias D, Penela D, Jáuregui B, et al. Cardiac magnetic resonance-guided ventricular tachycardia substrate ablation. *J Am Coll Cardiol EP*. 2020;6(4):436–447.

6. Priori SG, Blomström-Lundqvist C, Mazzanti A, et al. 2015 ESC Guidelines for the management of patients with ventricular arrhythmias and the prevention of sudden cardiac death: the task force for the management of patients with ventricular arrhythmias and the prevention of sudden cardiac death of the European Society of Cardiology (ESC). Endorsed by: Association for European Paediatric and Congenital Cardiology (AEPC). *Eur Heart J*. 2015;36(41):2793–2867.

7. Mäkikallio TH, Barthel P, Schneider R, et al. Prediction of sudden cardiac death after acute myocardial infarction: role of Holter monitoring in the modern treatment era. *Eur Heart J*. 2005;26(8):762–769.

8. Soto-Iglesias D, Acosta J, Penela D, et al. Image-based criteria to identify the presence of epicardial arrhythmogenic substrate in patients with transmural myocardial infarction. *Heart Rhythm*. 2018;15(6):814–821.

9. Andreu D, Ortiz-Perez JT, Fernandez-Armenta J, et al. 3D delayed enhancement magnetic resonance sequences improve conducting channel delineation prior to ventricular tachycardia ablation. *Eur Heart J*. 2013;34(suppl 1), 1915-1915.

10. Thiele H, Kappl MJE, Conradi S, Niebauer J, Hambrecht R, Schuler G. Reproducibility of chronic and acute infarct size measurement by delayed enhancement-magnetic resonance imaging. *J Am Coll Cardiol*. 2006;47(8):1641–1645.

11. Yan AT, Shayne AJ, Brown KA, et al. Characterization of the peri-infarct zone by contrast-enhanced cardiac magnetic resonance imaging is a powerful predictor of post-myocardial infarction mortality. *Circulation*. 2006;114(1):32–39.

12. Roes SD, Borleffs CJW, Van Der Geest RJ, et al. Infarct tissue heterogeneity assessed with contrast-enhanced MRI predicts spontaneous ventricular arrhythmia in patients with ischemic cardiomyopathy and implantable cardioverter-defibrillator. *Circ Cardiovasc Imaging*. 2009;2(3):183–190.

13. Chen Z, Sohal M, Voigt T, et al. Myocardial tissue characterization by cardiac magnetic resonance imaging using T1 mapping predicts ventricular arrhythmia in ischemic and non-ischemic cardiomyopathy patients with implantable cardioverter-defibrillators. *Heart Rhythm*. 2015;12(4):792–801.

14. Cuculich PS, Zhang J, Wang Y, et al. The electrophysiological cardiac ventricular substrate in patients after myocardial infarction: noninvasive characterization with electrocardiographic imaging. *J Am Coll Cardiol*. 2011;58(18):1893–1902.

15. Orini M, Graham AJ, Srinivasan NT, et al. Evaluation of the reentry vulnerability index to predict ventricular tachycardia circuits using high-density contact mapping. *Heart Rhythm*. 2020;17(4):576–583.

16. Graham AJ, Orini M, Zacur E, et al. Simultaneous comparison of electrocardiographic imaging and epicardial contact mapping in structural heart disease. *Circ Arrhythm Electrophysiol*. 2019;12(4):e007120.

17. Duchateau J, Sacher F, Pambrun T, et al. Performance and limitations of noninvasive cardiac activation mapping. *Heart Rhythm*. 2019;16(3):435–442.

18. Burnes JE, Taccardi B, Ershler PR, Rudy Y. Noninvasive electrocardiogram imaging of substrate and intramural ventricular tachycardia in infarcted hearts. *J Am Coll Cardiol*. 2001;38(7):2071–2078.

19. Cuculich PS, Schill MR, Kashani R, et al. Noninvasive cardiac radiation for ablation of ventricular tachycardia. *N Engl J Med*. 2017;377(24):2325–2336.

20. Wang L, Gharbia OA, Nazarian S, Horáček BM, Sapp JL. Non-invasive epicardial and endocardial electrocardiographic imaging for scar-related ventricular tachycardia. *Europace*. 2018;20(FI2):f263–f272.

21. Zhang J, Cooper DH, Desouza KA, et al. Electrophysiologic scar substrate in relation to VT: noninvasive high-resolution mapping and risk assessment with ECGI. *Pacing Clin Electrophysiol*. 2016;39(8):781–791.

22. Sosa E, Scanavacca M, D'Avila A, Pilleggi F. A new technique to perform epicardial mapping in the electrophysiology laboratory. *J Cardiovasc Electrophysiol*. 1996;7(6):531–536.

23. Marchlinski FE, Callans DJ, Gottlieb CD, Zado E. Linear ablation lesions for control of unmappable ventricular tachycardia in patients with ischemic and nonischemic cardiomyopathy. *Circulation*. 2000;101(11):1288–1296.

24. Orini M, Graham AJ, Martinez-Naharro A, et al. Noninvasive mapping of the electrophysiological substrate in cardiac amyloidosis and its relationship to structural abnormalities. *J Am Heart Assoc*. 2019;8(18):e012097.

25. Andrews CM, Srinivasan NT, Rosmini S, et al. Electrical and structural substrate of arrhythmogenic right ventricular cardiomyopathy determined using noninvasive electrocardiographic imaging and late gadolinium magnetic resonance imaging. *Circ Arrhythmia Electrophysiol*. 2017;10(7):e005105.

26. Coronel R, de Bakker JMT, Wilms-Schopman FJG, et al. Monophasic action potentials and activation recovery intervals as measures of ventricular action potential duration: experimental evidence to resolve some controversies. *Heart Rhythm*. 2006;3(9):1043–1050.

27. Orini M, Taggart P, Lambiase PD. In vivo human sock-mapping validation of a simple model that explains unipolar electrogram morphology in relation to conduction-repolarization dynamics. *J Cardiovasc Electrophysiol*. 2018;29(7):990–997.

28. Orini M, Srinivasan N, Graham AJ, Taggart P, Lambiase PD. Further evidence on how to measure local repolarization time using intracardiac unipolar electrograms in the intact human heart. *Circ Arrhythmia Electrophysiol*. 2019;12(11):e007733.

29. Campos FO, Orini M, Arnold R, et al. Assessing the ability of substrate mapping techniques to guide ventricular tachycardia ablation using computational modelling. *Comput Biol Med*. 2021;130:104214.

30. Martin CA, Orini M, Srinivasan NT, et al. Assessment of a conduction-repolarisation metric to predict arrhythmogenesis in right ventricular disorders. *Int J Cardiol*. 2018;271:75–80.

31. Graham AJ, Orini M, Zacur E, et al. Evaluation of ECG imaging to map haemodynamically stable and unstable ventricular arrhythmias. *Circ Arrhythmia Electrophysiol*. 2020;13(2):e007377.

32. Hutchinson MD, Gerstenfeld EP, Desjardins B, et al. Endocardial unipolar voltage mapping to detect epicardial ventricular tachycardia substrate in patients with nonischemic left ventricular cardiomyopathy. *Circ Arrhythmia Electrophysiol*. 2011;4(1):49–55.

33. Bear LR, Doz YS, Svehlikova J, et al. Effects of ECG signal processing on the inverse problem of electrocardiography. *Comput Cardiol (2010)*. 2018:45. https://doi.org/10.22489/CinC.2018.70

34. Karoui A, Bear L, Migerditichan P, Zemzemi N. Evaluation of fifteen algorithms for the resolution of the electrocardiography imaging inverse problem using ex-vivo and in-silico data. *Front Physiol*. 2018;9:1708. https://doi.org/10.3389/fphys.2018.01708

35. Takigawa M, Relan J, Kitamura T, et al. Impact of spacing and orientation on the scar threshold with a high-density grid catheter. *Circ Arrhythmia Electrophysiol*. 2019;12(9):e007158.

36. Glashan CA, Androulakis AFA, Tao Q, et al. Whole human heart histology to validate electroanatomical voltage mapping in patients with non-ischaemic cardiomyopathy and ventricular tachycardia. *Eur Heart J*. 2018;39(31):2867–2875.

37. Leong KMW, Ng FS, Shun-Shin MJ, et al. Non-invasive detection of exercise-induced cardiac conduction abnormalities in sudden cardiac death survivors in the inherited cardiac conditions. *Europace*. 2021;23(2):305–312.

38. Jamil-Copley S, Bokan R, Kojodjojo P, et al. Noninvasive electrocardiographic mapping to guide ablation of outflow tract ventricular arrhythmias. *Heart Rhythm*. 2014;11(4):587–594.

39. Orini M, Seraphim A, Graham A, et al. Detailed assessment of low-voltage zones localization by cardiac MRI in patients with implantable devices. *J Am Coll Cardiol EP*. 2022;8(2):225–235.

KEY WORDS **ECG imaging, electrogram, scar, ventricular tachycardia, voltage**

APPENDIX **For supplemental tables, please see the online version of this paper.**